

Haverford College

Haverford Scholarship

Faculty Publications

Chemistry

1997

The rotational spectrum and molecular properties of bromine dioxide, OBrO

Holger S. P. Muller

Charles E. Miller
Haverford College

Edward A. Cohen

Follow this and additional works at: https://scholarship.haverford.edu/chemistry_facpubs

Repository Citation

Müller, Holger SP, Charles E. Miller, and Edward A. Cohen. "The rotational spectrum and molecular properties of bromine dioxide, OBrO." *The Journal of chemical physics* 107 (1997): 8292.

This Journal Article is brought to you for free and open access by the Chemistry at Haverford Scholarship. It has been accepted for inclusion in Faculty Publications by an authorized administrator of Haverford Scholarship. For more information, please contact nmedeiro@haverford.edu.

The rotational spectrum and molecular properties of bromine dioxide, OBrO

Holger S. P. Müller, Charles E. Miller, and Edward A. Cohen

Citation: *J. Chem. Phys.* **107**, 8292 (1997); doi: 10.1063/1.475030

View online: <http://dx.doi.org/10.1063/1.475030>

View Table of Contents: <http://jcp.aip.org/resource/1/JCPSA6/v107/i20>

Published by the [American Institute of Physics](#).

Additional information on *J. Chem. Phys.*

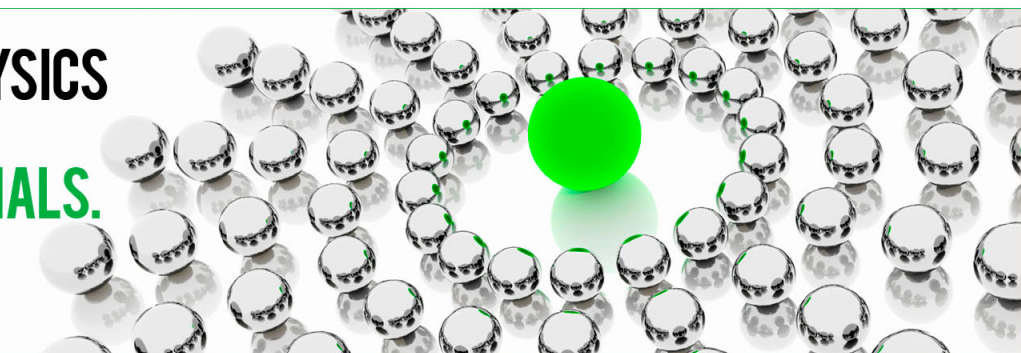
Journal Homepage: <http://jcp.aip.org/>

Journal Information: http://jcp.aip.org/about/about_the_journal

Top downloads: http://jcp.aip.org/features/most_downloaded

Information for Authors: <http://jcp.aip.org/authors>

ADVERTISEMENT



**ALL THE PHYSICS
OUTSIDE OF
YOUR JOURNALS.**

www.physics-today.org
**physics
today**

The rotational spectrum and molecular properties of bromine dioxide, OBrO

Holger S. P. Müller,^{a)} Charles E. Miller,^{b)} and Edward A. Cohen
Jet Propulsion Laboratory, California Institute of Technology, Pasadena, California 91109-8099

(Received 16 June 1997; accepted 19 August 1997)

The rotational spectrum of the OBrO radical has been observed in the gas phase over the solid products of the O+Br₂ reaction. Spectra have been measured for both O⁷⁹BrO and O⁸¹BrO in their (000), (010), and (020) vibrational states in selected regions between 88 and 627 GHz spanning the quantum numbers $1 \leq N \leq 61$ and $0 \leq K_a \leq 14$. The spectra are well described by a Hamiltonian which includes centrifugal distortion effects for fine and hyperfine terms. The molecular structure, the dipole moment, and the harmonic force field have been derived, and they, as well as fine and hyperfine structure constants, are compared with data of related molecules and electron spin resonance data from OBrO isolated in cryogenic salt matrices. © 1997 American Institute of Physics. [S0021-9606(97)01544-4]

I. INTRODUCTION

Current photochemical models suggest that catalytic cycles involving bromine oxides may account for up to 40% of the total stratospheric ozone depletion.¹ The molecular properties and chemical reactions of the BrO_x species included in these models are assumed to be similar to those of their ClO_x analogs. While the chemical and spectroscopic properties of chlorine oxides have been studied quite extensively in recent years, bromine oxides have been less well characterized.^{1,2} The recent detection of OBrO in the Br-sensitized photodecomposition of O₃ suggests the potential importance of this molecule in atmospheric reaction cycles.^{3,4}

Although Schwarz and Schmeißer first obtained bromine dioxide almost 60 years ago from a Br₂/O₂ discharge at low temperatures,⁵ further studies were sparse until very recently. Electron spin resonance (ESR) studies on x-ray irradiated perbromates provided some insight into the fine and hyperfine structure.⁶ Vibrational spectra were observed in Ar matrices.⁷⁻⁹ A mass spectrometric investigation of the O+Br₂ reaction system found evidence for a symmetric BrO₂ isomer, and from the comparison of electric focusing curves concluded that its dipole moment was similar to that of CH₂Cl₂, 1.6 D.¹⁰ Very recently, a combined spectroscopic and *ab initio* analysis of the $C^2A_2 \leftarrow X^2B_1$ visible absorption spectrum has yielded data for vibrational bands in the ground and excited electronic states.¹¹

As part of a program to provide a millimeter and submillimeter spectral data base of molecules with potential importance for the upper atmosphere and to derive molecular properties which may influence their chemical behavior, we have studied several bromine-oxygen compounds.¹²⁻¹⁵ In a recent communication we gave a preliminary account of our investigations of the millimeter and submillimeter spectra of

Br₂O and OBrO.¹⁴ These were the first high-resolution studies and structure determinations of polyatomic bromine oxides in the gas phase. In this article the spectra of two OBrO isotopomers in the ground state as well as the first and second excited bending states are described in detail together with the fitting procedure. The derived spectroscopic constants and molecular properties are discussed.

II. EXPERIMENT

The measurements were done using a 1 m long, 7.3 cm diameter, double-pass, temperature controlled glass cell. Phase-locked klystrons operating near 100 GHz were used as sources. Diode detectors were used for fundamental frequencies, and a liquid He-cooled InSb hot electron bolometer was used to detect harmonics. Further details of the spectrometer are given in Refs. 16 and 17. The regions 405.0–422.0 and 423.9–426.4 GHz were scanned in their entirety in order to facilitate the initial assignment process. Additional, selected measurements were made in the regions 398–432, 313–319, 88–96, and 626–627 GHz during the final stages of the analysis for the purpose of improving the precision of the derived molecular parameters.

The products of an O₂ discharge (~60 Pa) and Br₂ (1–4 Pa) were introduced into the absorption cell ($T \sim 250$ K) via separate sidearm inlets under slow flow conditions. An unidentified bromine oxide was condensed on the cell walls. After the flows of O₂ and Br₂ were stopped, the solid produced a clean and stable source of gas phase OBrO. With well-conditioned cell walls spectra could be recorded for an amount of time that was comparable to the deposition time, up to several hours.

At low temperatures, ~255 K, and low pressures, ~0.1 Pa, essentially all of the absorptions could be assigned to OBrO. Very weak features of BrO¹² indicated only traces of this radical to be present. At higher temperatures, ~260–270 K, and with pumping speed adjusted to maintain pressures in the 0.5–2 Pa region the intensity of OBrO lines increased.

^{a)}Present address: I. Physikalisches Institut, Universität zu Köln, Zùlpicher Str. 77, D-50937 Köln, Germany.

^{b)}Present address: Department of Chemistry, Haverford College, Haverford, Pennsylvania 19041.

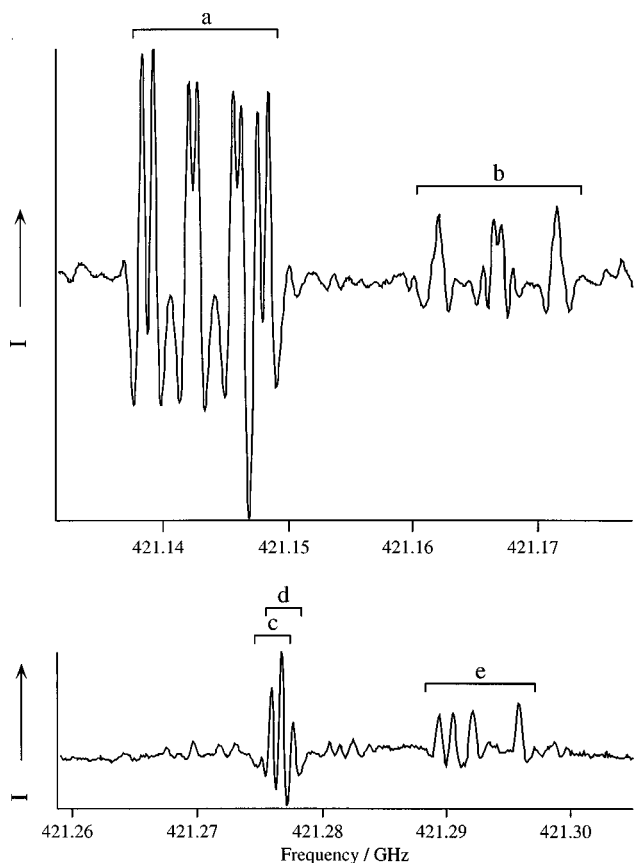


FIG. 1. Detail of the rotational spectrum of a mixture of bromine oxides over a condensate at -7°C and ca 1 Pa pressure. Some transitions are indicated: (a) ^{81}BrO , $^2\Pi_{3/2}$, $33/2-31/2$; (b) $^{79}\text{BrO}^{81}\text{Br}$, $v_2=1$, 26_6-25_5 ; (c) $^{81}\text{Br}_2\text{O}$, $93_{11}-94_{10}$; (d) $^{79}\text{BrO}^{81}\text{Br}$, $92_{11}-93_{10}$; (e) O^{81}BrO , $30_{11,20}-30_{10,21}$, $J=29.5$. Here BrO is about three orders of magnitude less abundant than Br_2O ; OBrO is about halfway between.

However, the intensity of BrO lines increased more rapidly, and lines of Br_2O^{15} were observed as well, as shown in Fig. 1.

For dipole measurements of OBrO two Stark plates were mounted inside the absorption cell. These plates consisted of 0.953 m long, 54.8 mm wide, and 6.35 mm thick aluminum bars which were 25.4 mm apart.

III. RESULTS

A. Observed spectra and assignment

OBrO is a moderately asymmetric, prolate top ($\kappa = -0.8246$) with its dipole moment along the b axis. Because of its C_{2v} symmetry, 2B_1 electronic ground state, and $I(^{16}\text{O})=0$, only rotational levels with K_a+K_c odd are allowed in the ground and totally symmetric vibrational states. The rotational, electron spin, and nuclear spin angular momenta are coupled in the following way:

$$\mathbf{N} + \mathbf{S} = \mathbf{J}, \quad (1)$$

$$\mathbf{J} + \mathbf{I}_{\text{Br}} = \mathbf{F}. \quad (2)$$

Therefore the electron spin-rotation coupling splits rotational levels into two, and each sublevel is further divided

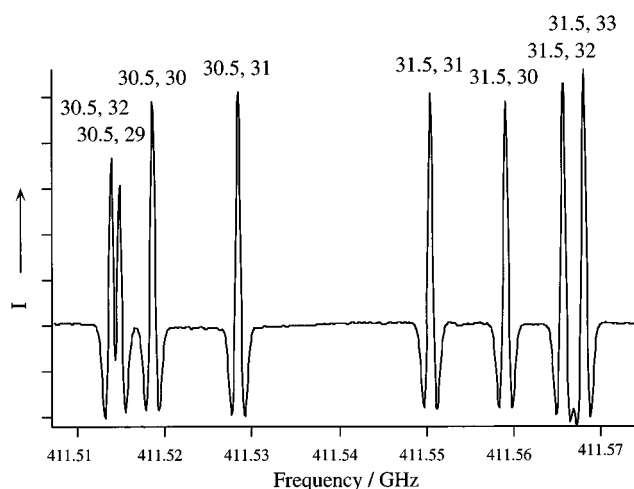


FIG. 2. The $32_{1,32}-31_{0,31}$ transition of O^{81}BrO in the ground vibrational state; the quantum numbers J, F of the lower state are indicated.

into four because of the magnetic and quadrupole interactions of the Br nuclei [$I(^{79}\text{Br})=I(^{81}\text{Br})=3/2$]. The majority of the observed transitions are the strongest of the allowed transitions, described by $\Delta F=\Delta J=\Delta N$. Thus a typical rotational transition appears as a doublet of quartets.

Initial simulations of the spectra were made using values for the electron spin-rotation, spin-spin, and nuclear quadrupole coupling constants derived from ESR measurements⁶ and structural parameters ($r_0=164.5$ pm and $\alpha_0=112.3^{\circ}$) and centrifugal distortion constants estimated from the related molecules OClO,^{18,19} SO_2 ,^{20,21} and SeO_2 .^{22,23}

In the first spectra recorded near 410 GHz, the strongest transitions are R -branch lines ($N+1 \leftarrow N$) with $N \approx 30$ and K_c between $N-2$ and N . These transitions have easily recognizable patterns for which all eight hyperfine components occur within 100 MHz. An example of one such group is shown in Fig. 2. Transitions having a constant value of $N-K_c$ have characteristic spacings of $\sim 2C$ for high N and $K_c \approx N$, making the identification of a series of related transitions straightforward. Further assignments proceeded quickly from this point for both O^{79}BrO and O^{81}BrO . Eventually it was possible to assign rotational transitions for which hyperfine splittings of more than 1 GHz and fine structure splittings of up to 5 GHz were observed. Selected OBrO ground-state transitions are given in Table I. Statistical information describing the observed transitions is shown in Table II.

A number of transitions for the $v_2=1$ vibrational state were identified based on the similarity of their patterns with those of the ground-state transitions, their relative intensity, and the consistency of the derived vibration-rotation interaction constants with those of OClO,¹⁸ SO_2 ,²¹ and SeO_2 .²² Finally, a substantial number of $v_2=2$ lines could also be assigned. The complete list of lines used in the final fit, their uncertainties, as well as their positions calculated from the

TABLE I. Observed frequencies (MHz) and assignments, uncertainties,^a (kHz) and residuals (kHz) (o-c) of selected rotational transitions of OBrO in the ground vibrational state.

$N'_{Ka',Kc'} - N''_{Ka'',Kc''}$ $J' + 1/2, F' - J'' + 1/2, F''$	uncertainties	o-c
O ⁷⁹ BrO		
15 _{3,12} -14 _{2,13}		
16,17-15,16	416333.837	50
16,16-15,15	416485.526	70
16,15-15,14	416711.478	50
16,14-15,13	416994.719	50
15,13-14,12	420349.572	50
15,14-14,13	420507.380	50
15,15-14,14	420753.428	70
15,16-14,15	421105.134	100
21 _{5,16} -21 _{2,19}		
22,23-22,23	418986.740	50
22,22-22,22	419086.474	50
22,21-22,21	419241.426	50
22,20-22,20	419443.649	50
9 _{5,4} -8 _{4,5}		
10,9-9,9	316707.654	40
10,10-9,10	316713.345	60
10,8-9,8	316717.878	60
10,11-9,10	316747.985	35
10,10-9,9	316748.657	35
10,9-9,8	316762.512	35
10,8-9,7	316785.046	35
9,8-8,7	318619.512	40
9,7-8,6	318620.868	40
9,9-8,8	318631.072	40
9,10-8,9	318661.232	40
6 _{6,1} -5 _{5,0}		
7,7-6,7	313939.875	60
7,8-6,7	313983.935	35
7,7-6,6	313985.513	35
7,6-6,5	313990.516	35
7,5-6,4	314005.964	35
7,6-6,6	314100.759	50
7,5-6,5	314204.936	80
6,6-5,6	316043.947	40
6,5-5,5	316231.612	40
6,5-5,4	316325.339	40
6,4-5,3	316327.484	40
6,6-5,5	316332.012	50
6,7-5,6	316337.083	50
6,4-5,4	316347.164	70
O ⁸¹ BrO		
2 _{2,1} -1 _{1,0}		
3,3-2,2	88860.912	35
3,4-2,3	88888.478	35
2,2-1,2	90310.681	30
2,3-1,2	90550.750	30
32 _{2,31} -31 _{1,30}		
32,33-31,32	424283.455	50
32,32-31,31	424286.881	50
32,31-31,30	424289.731	50
32,30-31,29	424291.737	50
33,31-32,30	424329.762	50
33,32-32,31	424334.074	50
33,33-32,32	424337.151	50
33,34-32,33	424340.981	50
48 _{2,47} -47 _{1,46}		
48,48-47,47	626252.640	150
48,47-47,46	626253.080	250

TABLE I. (Continued).

$N'_{Ka',Kc'} - N''_{Ka'',Kc''}$ $J' + 1/2, F' - J'' + 1/2, F''$	uncertainties	o-c
48,49-47,48 ^b	626253.640	100
48,46-47,45 ^b		
49,47-48,46 ^b	626299.351	120
49,49-48,48 ^b		
49,50-48,49	626304.764	80
13 _{2,11} -12 _{1,12}		
14,15-13,14	405675.283	50
14,14-13,13	405788.551	70
14,13-13,12	406325.869	50
14,12-13,11	406681.132	50
13,11-12,10	410542.900	150
13,12-12,11	410763.506	120
13,13-12,12	411089.913	50
30 _{14,17} -31 _{13,18}		
31,32-32,33	88302.114	20
31,31-32,32	88302.677	20
31,30-32,31	88311.211	20
31,29-32,30	88327.043	20
30,28-31,29	90201.802	35
30,29-31,30	90202.669	35
30,30-31,31	90211.278	50
30,31-31,32	90228.270	35

^a2σ confidence level.^bBlended lines. The residual is the intensity weighted average of the two lines.

final fit is available from the Electronic Physics Auxiliary Publication Service (E-PAPS) of the American Institute of Physics.²⁴ A machine-readable list of OBrO frequencies, intensities, and assignments in the ground vibrational state is available online in the JPL Submillimeter, Millimeter, and Microwave Line Catalog (<http://spec.jpl.nasa.gov>).²⁵

B. Analysis of the spectra

The OBrO Hamiltonian can be written as

$$\mathcal{H} = \mathcal{H}_{\text{rot}} + \mathcal{H}_{\text{fs}} + \mathcal{H}_{\text{hfs}}, \quad (3)$$

where \mathcal{H}_{rot} is a Watson S reduction of the rotational Hamiltonian in the I' representation which contains up to octic centrifugal distortion terms; \mathcal{H}_{fs} is a fine structure Hamiltonian describing the electron spin-rotation with up to sextic distortion terms; and \mathcal{H}_{hfs} is a hyperfine structure Hamiltonian which includes spin-spin coupling with quartic distortion terms, and nuclear quadrupole and nuclear spin-rotation coupling. This Hamiltonian is similar to the one used for OClO,¹⁹ however, additional distortion and nuclear spin-rotation coupling terms were required to fit the OBrO spectrum to within experimental uncertainties.

The quartic distortion terms for the A and S reduced Hamiltonians have been derived by Brown and Sears.²⁶ For an orthorhombic molecule such as OBrO, the terms in the S reduction and the representation I' are given by

$$\begin{aligned} \mathcal{H}_{\text{sr}}^{(4,S)} = & D_{N'}^s N^2 \mathbf{N} \cdot \mathbf{S} + D_{NK}^s (N^2 N_a S_a + N_a S_a N^2) / 2 \\ & + D_{KN}^s N_a^2 \mathbf{N} \cdot \mathbf{S} + D_K^s N_a^3 S_a + d_1^s (N_+^2 + N_-^2) \mathbf{N} \cdot \mathbf{S} \\ & + d_2^s (N_+^3 S_+ + N_-^3 S_-). \end{aligned} \quad (4)$$

TABLE II. Number of rotational levels, fine, and hyperfine structure components, and range of N and K_a quantum numbers in the final fit of OBrO.

	Ground state		$v_2=1$		$v_2=2$	
	O ⁷⁹ BrO	O ⁸¹ BrO	O ⁷⁹ BrO	O ⁸¹ BrO	O ⁷⁹ BrO	O ⁸¹ BrO
N_{rot}	82	92	41	40	15	17
N_{fs}	128	145	53	55	25	20
N_{hfs}	455	533	162	161	83	60
$N_{\text{min}}-N_{\text{max}}$	1-61	1-61	8-54	9-54	14-32	8-32
$K_{\text{min}}-K_{\text{max}}$	0-14	0-14	0-11	0-12	0-10	0-10

The corresponding reduced sextic Hamiltonian has not been derived, but the form of the quartic Hamiltonian suggests the following nine term expression may be appropriate:

$$\begin{aligned} \mathcal{H}_{\text{sr}}^{(6,s)} = & H_N^s N^4 \mathbf{N} \cdot \mathbf{S} + H_{\text{NNK}}^s (N^4 N_a S_a + N_a S_a N^4) / 2 \\ & + H_{\text{KNN}}^s N^2 N_a^2 \mathbf{N} \cdot \mathbf{S} + H_{\text{NKK}}^s (N^2 N_a^3 S_a \\ & + N_a^3 S_a N^2) / 2 + H_{\text{KKN}}^s N_a^4 \mathbf{N} \cdot \mathbf{S} + H_K^s N_a^5 S_a \\ & + h_1^s N^2 (N_+^2 + N_-^2) \mathbf{N} \cdot \mathbf{S} + h_2^s N^2 (N_+^3 S_+ + N_-^3 S_-) \\ & + h_3^s (N_+^5 S_+ + N_-^5 S_-). \end{aligned} \quad (5)$$

The completeness of the above expression has not been addressed, but there appear to be no redundant terms. Since the data set does not contain enough information for the determination of all nine sextic spin-rotation constants, various combinations of operators in the sextic Hamiltonian were used in trial fits of the data. The best fit utilized the last four terms of Eq. (5).

Predictions and fittings were done with Pickett's programs SPCAT and SPFIT.²⁷ The uncertainties attributed to individual transitions were in general one-tenth of the half-width; they were increased for lines with low signal-to-noise ratio or incompletely resolved lines. The uncertainties reflect a 2σ confidence level. Completely blended lines were fit as the intensity weighted average of their components. All parameters are positively defined, except for D_J , D_{JK} , and D_K .

For the $v_2=1$ state, changes $\Delta^1 C$ from the ground-state constants C_0 were defined as

$$\Delta^1 C = C_1 - C_0, \quad (6)$$

where C_1 designates $v_2=1$ spectroscopic constants. For the $v_2=2$ state changes from the ground state were in general assumed to be twice the value of those from the $v_2=1$ state. For some constants it was necessary to introduce second differences $\Delta^2 C$ which were defined as

$$\Delta^2 C = C_2 - C_0 - 2\Delta^1 C, \quad (7)$$

where C_2 designates $v_2=2$ spectroscopic constants. The (000), (010), and (020) states for both isotopomers were fit simultaneously in a single calculation. Some high-order parameters were common to both isotopomers or to different vibrational states. The ratios of some higher-order hyperfine constants were fixed to the isotopic ratios determined for the Br nuclei in atomic beam experiments.²⁸ For the highest-

order parameters, the present data justified using only a subset of the possible constants. In such cases, the choice of parameters may not be unique, but the effect on the lower-order parameters and their interpretation is insignificant. The final spectroscopic constants are presented in Tables III–V, and derived parameters are given in Table VI. The magnitudes of the centrifugal distortion constants vary in a regular way appropriate to the powers of the angular momentum operators, and the consistency of the parameters between the two isotopomers is excellent.

C. Dipole moment

The Stark effect measurements have been made under weak field conditions using the shifts of the intensity weighted averages of the unresolved Stark components. The measured shifts were proportional to the square of the applied fields as long as the shifts of the individual Stark components were within a linewidth of the intensity weighted average. Depending on the individual line, the largest shifts used in the fits were between ~ 150 and ~ 350 kHz. The $27_{3,25}-27_{2,26}$ transitions of SO₂ in the (000) and (010) states^{21,29} as well as several transitions of FClO₂ in the ground vibrational state³⁰ were used for calibration. While the results for SO₂ and FClO₂ agreed to $\sim 0.3\%$ the scatter of the measurements for each molecule and the uncertainties in the FClO₂ dipole moments cause an overall uncertainty of $\sim 2\%$ for the calibration.

The $15_{5,10}-14_{4,11}$ transition of O⁸¹BrO was chosen for the determination of the OBrO dipole moment. The rotational levels $15_{5,10}$ and $14_{6,9}$ are near-degenerate, their energy difference is -369 and 998 MHz for the $J'=13.5$ and 14.5 fine structure components, respectively. Thus only up to ~ 60 and ~ 115 V cm⁻¹ were needed in order to shift the individual hyperfine components up to ~ 350 kHz. Five hyperfine components could be used for the Stark measurements, all four in the case of $J'=13.5$, only the $F'=13$ component for $J'=14.5$. The remaining components were overlapped by or too close to other strong lines. The results of five Stark measurements were averaged and yielded a dipole moment of $2.81(10)$ D. The uncertainty reflects a 1σ confidence level, and it includes the uncertainty of the calibration.

TABLE III. Rotational and centrifugal distortion constants^a C (MHz) of OBrO in the (000) state, their changes $\Delta^1 C$ in the (010) state,^b and their second differences $\Delta^2 C$ in the (020) state.^b

C	O ⁷⁹ BrO	O ⁸¹ BrO	O ⁷⁹ BrO	O ⁸¹ BrO	O ⁷⁹ BrO	O ⁸¹ BrO
	Ground state		$v_2=1$		$v_2=2$	
A	28 024.518 21 (108)	27 824.890 96 (113)	493.095 4 (35)	488.976 8 (37)	19.5041 (83)	19.2756 (51)
B	8 233.172 826 (246)	8 233.254 666 (229)	-4.924 11 (122)	-4.946 71 (123)	-0.217 94 (153)	-0.215 96 (161)
C	6 345.433 279 (257)	6 335.136 755 (270)	-15.923 07 (138)	-15.884 17 (139)	-0.051 59 (48)	-0.050 56 (52)
$D_N \cdot 10^3$	7.135 185 (192)	7.125 027 (185)	-0.043 67 (170)			
$D_{NK} \cdot 10^3$	-70.691 69 (303)	-69.980 26 (298)	-2.4689 (49)	-2.4379 (50)	-0.1652 (70)	
$D_K \cdot 10^3$	714.3784 (225)	704.3855 (231)	67.768 (62)	66.775 (62)	6.919 (58)	6.638 (49)
$d_1 \cdot 10^3$	-2.637 561 (103)	-2.642 166 (103)	-0.007 771 (260)			
$d_2 \cdot 10^3$	-0.156 557 (51)	-0.156 820 (52)	-0.029 759 (99)		-0.000 973 (149)	
$H_N \cdot 10^7$	0.174 49 (48)		0.0029 (78)			
$H_{NK} \cdot 10^7$	-3.3992 (168)	-3.4210 (172)	-0.1619 (134)			
$H_{KN} \cdot 10^7$	-59.236 (201)	-57.780 (173)	-8.23 (41)			
$H_K \cdot 10^7$	610.37 (182)	597.67 (184)	123.6 (34)			
$h_1 \cdot 10^7$	0.092 95 (76)		-0.001 30 (101)			
$h_2 \cdot 10^7$	0.009 66 (53)		0.001 24 (63)			
$h_3 \cdot 10^7$	0.009 365 (109)		0.002 218 (133)			
$L_{NK} \cdot 10^{12}$	15.6 (88)					
$L_{KKN} \cdot 10^{12}$	874.0 (81)					
$L_K \cdot 10^{12}$	-7023.0 (510)					
$l_1 \cdot 10^{12}$	-0.0443 (167)					
$l_2 \cdot 10^{12}$	0.0045 (125)					
$l_3 \cdot 10^{12}$	-0.0073 (59)					
$l_4 \cdot 10^{12}$	-0.004 69 (138)					

^aNumbers in parentheses are two standard deviations in units of the least significant figures. One entry for both O⁷⁹BrO and O⁸¹BrO indicates common constants for both isotopomers.

^bSee Sec. III B.

D. Structural parameters and harmonic force field

The OBrO ground-state effective structure (r_0) can be calculated from any two of the three moments of inertia or the a - and b -planar moments for each of the isotopic species; the latter is given in Table VII. The uncertainties of the rotational constants are very small, so that the structural parameters calculated from any choice of moments for the two isotopomers agree to much better than the quoted figures.

However, the accuracy of the r_0 structural parameters is limited by vibrational effects which lead to different values depending on the choice of moments. The uncertainties ascribed to them in Table VII have been chosen to cover the range of values calculated from any choice of two moments.

The r_0 structure was used for the initial calculation of the harmonic force field, which is described below. The harmonic contributions to the α constants were then derived for

TABLE IV. Fine structure constants^a C (MHz) of OBrO in the (000) state, their changes $\Delta^1 C$ in the (010) state,^b and their second differences $\Delta^2 C$ in the (020) state.^b

C	O ⁷⁹ BrO	O ⁸¹ BrO	O ⁷⁹ BrO	O ⁸¹ BrO	O ⁷⁹ BrO	O ⁸¹ BrO
	Ground state		$v_2=1$		$v_2=2$	
ϵ_{aa}	-2 352.219 2 (157)	-2 335.506 1 (159)	45.548 (38)	45.134 (40)	6.907 (75)	7.025 (70)
ϵ_{bb}	-565.664 4 (56)	-565.662 8 (49)	1.3519 (223)	1.3566 (211)	0.044 (65)	
ϵ_{cc}	52.574 1 (60)	52.485 8 (55)	0.4937 (187)	0.4989 (179)	0.0445 (233)	
$D_N^S \cdot 10^3$	-0.372 46 (269)		-0.0183 (73)			
$D_{NK}^S \cdot 10^3$	-0.624 5 (275)		0.607 (161)			
$D_{KN}^S \cdot 10^3$	-0.305 (34)		0.561 (191)			
$D_K^S \cdot 10^3$	-17.205 (191)	-16.791 (177)	-16.46 (37)			
$d_1^S \cdot 10^3$	-0.343 27 (204)		0.001 18 (230)			
$d_2^S \cdot 10^3$	-0.115 08 (108)		0.007 75 (95)			
$H_K^S \cdot 10^7$	37.6 (60)					
$h_1^S \cdot 10^7$	0.002 12 (95)					
$h_2^S \cdot 10^7$	0.001 42 (72)					
$h_3^S \cdot 10^7$	-0.000 748 (154)					

^aNumbers in parentheses are two standard deviations in units of the least significant figures. One entry for both O⁷⁹BrO and O⁸¹BrO indicates common constants for both isotopomers.

^bSee Sec. III B.

the calculation of the ground-state average structure (r_z). See Table VI for the B_z^i . Finally, the equilibrium structure (r_e) was estimated using Kuchitsu's relationship³¹

$$r_e = r_z - 3/2a\langle u^2 \rangle + K. \quad (8)$$

Here $\langle u^2 \rangle$ and K are the zero-point mean-square amplitude of the BrO bond and its perpendicular amplitude correction, respectively, calculated from the harmonic force field. The Morse anharmonicity constant $a = 1.976 \text{ \AA}^{-1}$ is taken from the BrO radical.¹² The initial r_e value is then used to refine the force field, and the procedure is repeated. In this model, ground-state average and equilibrium bond angles are assumed to be equal. It has been shown for Cl₂O that the ClO bond length calculated according to Eq. (8) agrees very well with the value determined from equilibrium rotational constants.¹⁵ For OClO, however, the bond length derived from Eq. (8) is ~ 0.2 pm longer than the one determined from equilibrium rotational constants, and in Table VII it is shown that the equilibrium bond angle is about 0.08° smaller than the ground-state average value. The OBrO equilibrium bond length has been calculated according to Eq. (8). The bond length and angle have been corrected by assuming similar deviations to those of OClO. The resulting r_e structure is given in Table VII; data for SeO₂ and SO₂ are also included for comparison purposes.

The harmonic force field has been calculated using Christen's program NCA.³⁵ The input parameters are given in Table VIII. The ν_3 isotopic shifts were corrected for the differences between gas phase and argon matrix positions, $\sim 3.4 \text{ cm}^{-1}$. Harmonic wave numbers were estimated³⁶ using the OClO values of $\omega_i/\nu_i = 1.02, 1.01, \text{ and } 1.02$ for $i = 1, 2, \text{ and } 3$.³⁷ The ground-state quartic distortion constants and the

inertial defect differences for $\nu_2 = 1$ and 2, obtained in the present study, were also used in the force field calculation.

The input data were weighted inversely to the squares of their attributed uncertainties: One-hundred times the experimental values were used for the quartic distortion constants, 1 cm^{-1} and 0.3 cm^{-1} for the vibrational wave numbers and isotopic shifts, respectively, and three times the experimental uncertainties were used for the inertial defect differences. The resulting force constants are given in Table IX together with values for related molecules. More than 99% of the potential-energy distribution of the vibrational modes is due to f_r and f_α , respectively. A comparison of the input data with values calculated from the force field is given in Table VIII.

IV. DISCUSSION

A. Structure, harmonic force field, and dipole moment

It is shown in Table VIII that the present force field reproduces the input data very well. Initially, the position of the ν_2 mode of O⁷⁹BrO was predicted to be at 311 cm^{-1} ,¹⁴ and the present force field yields a value of 313.3 cm^{-1} . This is in good agreement with measurements of 317.0 cm^{-1} for OBrO isolated in an argon matrix,⁹ and with a gas phase value of $317.5 \pm 3 \text{ cm}^{-1}$ obtained from an analysis of hot bands in the visible OBrO spectrum,¹¹ and with the relative intensities of the excited state rotational spectra.

The structural parameters agree very well with those from *ab initio* calculations. These are compared in Table VII. A comparison of the OBrO structure with those of related molecules is given in Table X. The trends observed among the dioxides of Br, Cl, Se, and S show great consistency. In

TABLE V. Spin-spin, nuclear quadrupole, and nuclear spin-rotation coupling constants^a C (MHz) of OBrO in the (000) state and their changes $\Delta^1 C$ in the (010) state.^b

C	O ⁷⁹ BrO	O ⁸¹ BrO	O ⁷⁹ BrO	O ⁸¹ BrO
	Ground state		$\nu_2 = 1$	
a_F	88.950 (30)	95.900 (32)	0.379 (121) ^c	0.408 (130) ^c
$a_F^J \cdot 10^3$	0.1262 (260) ^c	0.1360 (280) ^c		
$a_F^K \cdot 10^3$	-2.706 (276) ^c	-2.916 (298) ^c		
T_{aa}	-373.336 (47)	-402.452 (48)	-0.095 (78) ^c	-0.102 (84) ^c
$T_{aa}^J \cdot 10^3$	-0.211 (91) ^c	-0.227 (98) ^c		
$T_{aa}^K \cdot 10^3$	2.88 (42) ^c	3.11 (45) ^c		
T_-^d	-1 189.804 (42)	-1 282.545 (41)	0.942 (117) ^c	1.015 (126) ^c
$T_-^J \cdot 10^3$	0.979 (40) ^c	1.055 (43) ^c		
$T_-^K \cdot 10^3$	-46.38 (240) ^c	-49.99 (259) ^c		
χ_{aa}	356.221 (65)	297.587 (65)	0.354 (189) ^c	0.296 (158) ^c
χ_-^e	400.456 (95)	334.477 (92)	1.067 (260) ^c	0.892 (217) ^c
$C_{aa} \cdot 10^3$	160.12 (267)	167.52 (283)		
$C_{bb} \cdot 10^3$	41.58 (172)	42.32 (192)		
$C_{cc} \cdot 10^3$	31.65 (178)	31.89 (198)		

^aNumbers in parentheses are two standard deviations in units of the least significant figures. One entry for both O⁷⁹BrO and O⁸¹BrO indicates common constants for both isotopomers.

^bSee Sec. III B.

^cIsotopic ratio fixed, see Sec. III B.

^d $T_- = T_{bb} - T_{cc}$.

^e $\chi_- = \chi_{bb} - \chi_{cc}$.

TABLE VI. Rotational constants, vibration–rotation interaction constants,^a ground-state average rotational constants (MHz), and inertial defects (amu Å²).^b

	O ⁷⁹ BrO	O ⁸¹ BrO
A_{000}	28 024.518 21 (108)	27 824.890 96 (113)
B_{000}	8 233.172 826 (246)	8 233.254 666 (229)
C_{000}	6 345.433 279 (257)	6 335.136 755 (270)
Δ_{000}	0.227 801 5 (24)	0.228 478 8 (26)
A_{010}	28 517.613 6 (35)	28 313.867 8 (37)
B_{010}	8 228.248 71 (121)	8 228.307 96 (122)
C_{010}	6 329.510 21 (138)	6 319.252 58 (138)
Δ_{010}	0.703 243 0 (119)	0.705 767 8 (120)
A_{020}	29 030.213 2 (109)	28 822.120 2 (83)
B_{020}	8 223.106 66 (261)	8 223.145 28 (260)
C_{020}	6 313.535 56 (287)	6 303.317 85 (286)
Δ_{020}	1.179 780 5 (331)	1.184 136 2 (313)
$\alpha_2^A(\text{eff})^c$	-473.591 3 (89)	-469.7013 (68)
$\alpha_2^B(\text{eff})$	4.706 17 (212)	4.730 74 (222)
$\alpha_2^C(\text{eff})$	15.871 48 (139)	15.833 61 (144)
γ_{22}^A	9.752 1 (42)	9.6378 (26)
γ_{22}^B	-0.108 97 (76)	-0.107 98 (80)
γ_{22}^C	-0.025 79 (24)	-0.025 28 (26)
A_z	27 823.194 8	27 625.560 4
B_z	8 213.279 99	8 213.360 08
C_z	6 341.306 72	6 331.030 90

^aTerms of higher order than v^2 are neglected.

^bNumbers in parentheses are two standard deviations in units of the least significant figures.

^c $\alpha_2(\text{eff}) = \alpha_2 - \gamma_{12}/2 - \gamma_{23}/2$.

going from the third to the fourth row central atom, the lengthening of the bonds of the molecules in Table X is accompanied by a decrease in the stretching force constants. However, the changes in bond length and strength are not uniform as one proceeds from the singly bonded BrOBr to

OBrO. For the series XO₂, XO, and OXO, the bond lengths increase by 14.2, 15.1, and 17.1 pm, respectively, in going from Cl to Br. The corresponding ratios of stretching force constants are 0.974, 0.879, and 0.775, showing that multiply bonded Br forms weaker multiple bonds than does Cl. The longer and weaker bonds in the Br molecules can be explained by less efficient π bonding to the small O atom than is possible in the Cl compounds. As is expected the bond angles increase from OBrO to OClO and from SeO₂ and SO₂. Interestingly, the angle increases from OClO to SO₂, but it decreases slightly from OBrO to SeO₂.

As can be seen in Table VII, the dipole moment from an *ab initio* calculation is in good agreement with the present experimental value of 2.81 D. Both are in disagreement with the value of ~ 1.6 D from an electric focusing experiment.¹⁰ The OBrO dipole moment is slightly larger than that of SeO₂. A similar relationship exists between the dipole moments of OClO and SO₂.

B. Electron spin-rotation coupling constants

It is shown in Table IV that the electron spin-rotation constants are large, and they are precisely determined. In Table XI the consistency of the constants is demonstrated by the fact that the $\Lambda_{ii}^e = \epsilon_{ii}/B_i$ are virtually identical for both O⁷⁹BrO and O⁸¹BrO.

Since the electron spin–rotation constants are proportional to the rotational constants, it is more appropriate to compare values of Λ_{ii}^e . Despite the differences in π bonding between OBrO and OClO, pointed out in the previous section, the ratios of Λ_{aa}^e and Λ_{bb}^e are very similar. This is expected for planar radicals with ²B₁ symmetry in the ground electronic state.⁴¹ Ideally, the *cc*-components of the

TABLE VII. Structural parameters (pm, deg.) and dipole moment^a (D) of OBrO and related molecules.

Parameter	OBrO, experimental ^b			<i>ab initio</i> equilibrium structure			SeO ₂
	r_0	r_z	r_e^c	UMP2 ^d	CCSD(T) ^d	CCSD(T) ^e	r_e
r	164.91 (15)	164.968 (1)	164.4	164.0	165.0	166.0	160.76 ^f
α	114.44 (25)	114.429 (1)	114.3	115.4	114.9	114.8	113.83 ^f
μ	2.81 (10)			2.61			2.62 ^g
Parameter	OClO, experimental			<i>ab initio</i> equilibrium structure			SO ₂
	r_0	r_z	r_e^c	UMP2 ^d	CCSD(T) ^d	CCSD(T) ^e	r_e
r	147.49 ^h	147.556 ^h	146.984 ^j	148.5			143.08 ^k
α	117.49 ^h	117.485 ^h	117.403 ^j	117.9			119.33 ^k
μ	1.792 ⁱ			1.95			1.633 ^l

^aGround vibrational state.

^bThis work; numbers in parentheses are one standard deviation in units of the least significant figures.

^cDerived from r_z , see text.

^dReference 32. Unrestricted Møller–Plesset second order theory, UMP2, and coupled cluster with single, double, and perturbative treatment of triple excitations, CCSD(T), using triple zeta type basis sets with polarization functions.

^eReference 11. See previous footnote.

^fReference 22.

^gReference 33.

^hThis work, ground-state rotational constants from Ref. 19.

ⁱReference 34.

^jReference 18.

^kReference 20.

^lReference 29.

TABLE VIII. Comparison of experimental spectroscopic constants (cm^{-1} , kHz, $\text{amu} \text{ \AA}^2$) with those calculated from the force field.

parameter	O^{79}BrO		O^{81}BrO		$^{18}\text{O}^{79}\text{Br}^{18}\text{O}$		$^{18}\text{O}^{81}\text{Br}^{18}\text{O}$	
	obs.	calc.	obs.	calc.	obs.	calc.	obs.	calc.
$(\Delta) \omega_1^a$	811.6 ^b	806.3	-1.1 ^b	-1.19	-40.9 ^b	-40.53	-42.3 ^b	-41.79
$(\Delta) \omega_2^a$	320.0 ^b	316.4	-0.7 ^b	-0.66	-15.2 ^b	-15.04	-15.9 ^b	-15.72
$(\Delta) \omega_3^a$	865.6 ^c	867.9	-2.5 ^c	-2.39	-38.4 ^b	-38.42	-40.8 ^b	-40.92
D_J	7.135	7.168	7.125	7.159		5.700		5.691
D_{JK}	-70.69	-70.14	-69.98	-69.45		-58.20		-57.58
D_K	714.4	694.5	704.4	684.8		587.9		579.0
d_1	-2.638	-2.637	-2.642	-2.642		-2.064		-2.068
d_2	-0.1566	-0.1397	-0.1568	-0.1398		-0.1096		-0.1098
$\Delta\Delta_{010}$	0.4754	0.4722	0.4773	0.4740		0.4912		0.4936
$\Delta\Delta_{020}$	0.9520	0.9443	0.9556	0.9480		0.9824		0.9866

^a ω_i for O^{79}BrO ; $\Delta\omega_i := \omega_i(\text{OBrO}) - \omega_i(\text{O}^{79}\text{BrO})$ else; see also text. Input data from this work unless stated otherwise.

^bReference 9.

^cReference 14.

spin-rotation tensor should be zero for the planar OBrO and OCIO radicals.⁴¹ However, Λ_{cc}^e is small and negative for both molecules. This fact may be the result of higher-order effects, such as spin polarization or influences of multiple excitations.⁴¹ Since these effects are dominant in determining the value of Λ_{cc}^e , it should not be surprising that these values do not follow the simple relationships exhibited by the *aa* and *bb* components of the OBrO and OCIO.

The magnitude of the fine structure constants of radicals can be related to the fine structure intervals *A* of the atoms involved.^{41,42} The ratio between the ^{79}Br and ^{35}Cl atomic fine structure intervals is 4.19.^{41,42} Because only about half of the spin-density is on the X atom for OXO (cf. Sec. IV C) and because the fine structure interval for ^{16}O is much smaller than those of ^{79}Br and ^{35}Cl , the ratios of Λ_{aa}^e and Λ_{bb}^e are about 3.15. For the XO radicals only about one-third of the spin-density is on the halogen atom,¹² the ratio of the spin-orbit coupling constants⁴³ is consequently even smaller, 3.02.

In general, the *A* rotational constant increases markedly upon excitation of the bending mode for a molecule with C_{2v} symmetry. Although the number of examples is rather limited, among them $\text{H}_2\text{O}^+(^2B_1)$,⁴⁴ $\text{NH}_2(^2B_1)$,⁴⁵ $\text{CH}_2(^3B_1)$,⁴⁶ and $\text{NO}_2(^2A_1)$,⁴⁷ it appears as if the absolute value of ϵ_{aa} usually increases as well.⁴² However, the magnitude of ϵ_{aa} decreases upon excitation of ν_2 for both OBrO and OCIO.¹⁸ The second-order expression for ϵ_{ij} is^{41,48}

$$\epsilon_{ij} = -2\hbar^2 \sum_n \text{Re} \langle 0 | \mu_{ii} L_i | n \rangle \langle n | A_{SO} L_j | 0 \rangle / (E_0 - E_n), \quad (9)$$

where μ_{ii} denotes the *ii* component of the inverse inertia tensor, L_i is the *i*th component of the orbital angular momentum, A_{SO} of the molecule is approximated by the average of A_{SO} of the atoms in the molecules weighted according to the spin density at the atoms, and $|0\rangle$ and $|n\rangle$ are ground- and excited-state wave functions at energies E_0 and E_n , respectively. According to *ab initio* calculations for OCIO $E_0 - E_n$ decreases with excitation of the bending modes for the three lowest excited electronic states.⁴⁹ In order for ϵ_{aa} of OCIO to decrease substantially in magnitude with excitation

of the bending mode the numerator of Eq. (9) has to decrease. An analogous situation can be expected for OBrO.

The series of vibration-rotation interaction terms defined in Eqs. (6) and (7), which have been determined for the rotational constants in the bending mode, decrease faster than the analogous series of vibration-rotation interaction constants for the spin-rotation constants for both OBrO and OCIO. This is in accord with other C_{2v} radicals.

The data is of sufficient quality that quartic and even some sextic spin-distortion terms are well determined in the ground vibrational state. The changes upon excitation of the bending mode are of the same order of magnitude as the ground-state constants themselves for the three *K*-dependent diagonal quartic terms.

Information on the fine and hyperfine structure of a radical can be obtained not only from high-resolution spectroscopy but also from ESR studies. Curl has proposed a relationship between the electron spin-rotation constants ϵ_{ii} , obtained from high-resolution spectroscopy, and the electronic *g* values g_{ii} , obtained from ESR experiments:⁴⁸

$$-\epsilon_{ii}/2B_i = -\Lambda_{ii}^e/2 = g_{ii} - g_e, \quad (10)$$

where the B_i are the rotational constants and g_e is the *g* value of the free electron. In most ESR experiments OBrO was obtained by x-ray irradiation of perbromates in perbromate or perchlorate matrices.⁶ The results collected in Table XII show good agreement between the gas-phase constants

TABLE IX. Harmonic force constants (N m^{-1}) of OBrO and related molecules.

	OBrO ^a	OCIO ^b	SeO ₂ ^c	SO ₂ ^d
f_r	546.9	705.5	705.7	1064.3
f_α	102.6	138.2	135.7	169.7
f_{rr}	-5.0	-19.3	12.9	1.6
$f_{r\alpha}$	-6.1	1.8	13.8	25.2

^aThis work.

^bReference 18.

^cReference 38.

^dReference 20.

TABLE X. Comparison of structural parameters^a (pm, deg.) and force constants (N m⁻¹) of selected bromine oxides with those of related molecules.

	BrOBr ^b	ClOCl ^c	BrO ^d	ClO ^e	OBrO ^f	OCIO ^g	SeO ₂ ^h	SO ₂ ⁱ
<i>r</i>	183.79	169.59	172.07	156.96	164.4	146.98	160.76	143.08
Δr		14.20		15.11		17.4		17.68
<i>f_r</i>	287.4	294.8	412.7	469.4	546.9	705.5	705.7	1064.3
α	112.25	110.88			114.3	117.40	113.83	119.33
<i>f_α</i>	101.7	123.6			102.6	138.2	135.7	169.7

^a*r_e* parameter; estimates for Br₂O and OBrO.^bReference 15.^cReference 39.^dReference 12.^eReference 40.^fThis work.^gReference 18.^hReferences 22 and 38.ⁱReferences 20.

and the ESR data. A substantial amount of the differences may be attributable to perturbations of the electronic structure of the radical by the matrix. Recent *g* values for OCIO isolated in sulfuric acid glass,⁵⁰ which are given in Table XII, agree within the quoted figures with the gas-phase measurements.

C. Spin–spin coupling constants

It is shown in Table V that the spin–spin coupling constants and most of their quartic distortion terms have been precisely determined. As is demonstrated in Table XI, the ^{79/81}Br isotopic ratios obtained for *a_F*, *T_{aa}*, and *T₋* = *T_{bb}* – *T_{cc}* are in very good agreement with the ratio of the nuclear *g* values of the Br atoms. The matrix ESR measurements are in good agreement with the present results. The absolute values of *a_F* and *T_{ii}* from Ref. 6 are 3.0% to 7.2% larger than those of the gas phase O⁷⁹BrO molecule.

The spin–spin coupling constants are commonly interpreted in terms of spin-density of the unpaired electron in the valence shell of a given nucleus by comparing them with the coupling constants of the atom.^{41,51} The isotropic coupling constant, or Fermi contact term, *a_F* = 88.950(30) MHz for O⁷⁹BrO, indicates an almost negligible 4*s* character, 0.28%, for the unpaired electron. The interpretation in terms of a precise percentage of *s* character should be viewed cau-

tiously because higher-order effects, such as spin polarization, may contribute significantly to the magnitude of such a small *a_F*. The anisotropic coupling tensor [*T_{aa}* = –373.336(47), *T_{bb}* = –408.234(28), and *T_{cc}* = 781.570(35) MHz for O⁷⁹BrO] can be decomposed into two axially symmetric tensors, represented by their diagonal elements *z*, –*z*/2, –*z*/2 and –*y*/2, –*y*/2, *y*, respectively. The values *y* = 793.20 and *z* = 23.26, obtained from the anisotropic spin–spin coupling tensor, imply about 48.5% of the spin-density is perpendicular to the molecular plane in the 4*p_y* orbital and only ~1.4% is in the 4*p_z* orbital. The results for OCIO are quite similar in spite of the larger degree of π bonding in OCIO: 0.81% 3*s*, 1.0% 3*p_z*, and 46.3% 3*p_y*. Matrix ESR experiments with ¹⁷O enriched OCIO indicate that the remaining spin-density is essentially in the oxygen *p_y* orbitals,⁵² as expected for a π radical.

As can be seen in Table V, the constant *a_F* increases upon excitation of the bending mode. Within the model mentioned above, this indicates that the Br 4*s* character of the unpaired electron increases by about 0.001%. However, the changes in the anisotropic coupling tensor show that the percentages of *p_y* and *p_z* characters decrease by 0.038% and 0.013%, respectively, indicating a net loss of spin-density at the Br atom with excitation of the bending mode. The *K* dependences of the spin–spin coupling constants are in accord with the observed vibrational changes.

D. Nuclear quadrupole coupling constants

The ^{79/81}Br isotopic ratios for χ_{aa} and χ_{-} = χ_{bb} – χ_{cc} obtained from the submillimeter spectrum agree very well

TABLE XI. Isotopic ratios ^{79/81}C of fine and hyperfine constants of OBrO.

<i>C</i>	observed	expected/theoretical ^a
Λ_{aa}^e ^b	0.999 982 (10)	1.0
Λ_{bb}^e	1.000 013 (13)	1.0
Λ_{cc}^e	1.000 057 (155)	1.0
<i>a_F</i>	0.927 529 (440)	0.927 699 0 (2)
<i>T_{aa}</i>	0.927 653 (161)	0.927 699 0 (2)
<i>T₋</i>	0.927 690 (44)	0.927 699 0 (2)
χ_{aa}	1.197 03 (34)	1.197 056 8 (15)
χ_{-}	1.197 26 (44)	1.197 056 8 (15)
Λ_{aa}^n ^c	0.949 (24)	0.927 699 0 (2)
Λ_{bb}^n	0.983 (61)	0.927 699 0 (2)
Λ_{cc}^n	0.991 (84)	0.927 699 0 (2)

^aNeglecting vibrational effects.^b $\Lambda_{ii}^e = \epsilon_n / B_i$.^c $\Lambda_{ii}^n = C_{ii} / B_i$.TABLE XII. Comparison of electron spin–rotation coupling constants, electronic *g* values, and ratio of Λ_{ii}^e for OBrO and OCIO.

<i>i</i>	O ⁷⁹ BrO		O ³⁵ ClO		⁷⁹ Br/ ³⁵ Cl
	$\Lambda_{ii}^e/2^a$	<i>g_{ii}</i> – <i>g_e</i> ^{b,c}	$\Lambda_{ii}^e/2^d$	<i>g_{ii}</i> – <i>g_e</i> ^{b,e}	$\Lambda_{ii}^e(\text{OXO})$
<i>A</i>	0.0420	0.0512	0.0133	0.0133	3.1486
<i>B</i>	0.0344	0.0302	0.0109	0.0109	3.1513
<i>C</i>	–0.0041	–0.0062	–0.0003	–0.0003	15.17

^aThis work.^bMatrix ESR.^cReference 6.^dReference 19.^eReference 50.

TABLE XIII. Quadrupole coupling constants (MHz) of O⁷⁹BrO and O³⁵ClO and relative field gradient at the X nucleus.

	O ⁷⁹ BrO ^a	O ³⁵ ClO ^b
χ_{aa}	356.221 (65)	-52.086 (102)
χ_{bb}	22.118 (53)	2.808 (66)
χ_{cc}	-378.339 (62)	49.278 (66)
f_a^c	0.4628	0.475
f_b^c	0.0287	-0.026
f_c^c	-0.4915	-0.449

^aThis work.^bReference 19.^c $f_i = \chi_{ii}(\text{OXO})/eQq_{n10}(X)$.

with the ratio of the nuclear quadrupole constants of the Br atoms, as can be seen in Table XI. The diagonal elements of the quadrupole tensor of matrix-isolated O⁷⁹BrO from Ref. 6 deviate between less than 1 and ~10 MHz from those of the free molecule.

In spite of the changes in π bonding between OBrO and OClO, discussed in the structure and force field section, the relative field gradients at the X nuclei, which are given in Table XIII, are very similar, particularly along the a axis. Small differences occur along the c axis; the relative changes are more pronounced along the b axis because these components are rather small. Modified extended Hückel calculations yielded reasonable values for the quadrupole coupling constants of O⁷⁹BrO: 360, -15, and -345 MHz for χ_{aa} , χ_{bb} , and χ_{cc} , respectively,⁵³ compared to experimental values of 356, 22, and -378 MHz. In Ref. 53 it was found that the calculated constants are strongly dependent on changes in the bond length, and they are affected to a lesser extent by changes in the bond angle; 162.5 pm and 117.6° were assumed for the OBrO geometry.⁵³ Using our estimate of $r_e = 164.4$ pm and $\angle_e = 114.3^\circ$ and their calculated derivatives of the quadrupole constants,⁵³ values of 351, 0, and -351 MHz are obtained, in better agreement with experiment.

E. Nuclear spin-rotation constants

Although the effects of the nuclear spin-rotation coupling are in general very small, the respective spectroscopic constants have been precisely determined for OBrO. The ^{79/81}Br isotropic ratios of $\Lambda_{ii}^n = C_{ii}/B_i$ agree well with the ratio of the magnetic dipole moments of the Br atoms, as is shown in Table XI. Because the nuclear spin-rotation con-

TABLE XIV. Ratios of spin-rotation and rotational constants ($C_{ii}^0/B_i^0 \times 10^6$) of O⁷⁹BrO and related molecules.

i	OBrO ^a	BrO ^b	Br ₂ O ^c	HOBr ^d	BrF ^e	BrCl ^f	BrNO ^g	CH ₃ Br ^h	HBr ⁱ
a	5.72	...	1.3	0.1	2.43	0.119	...
b	5.06	5.4	6.1	5.7	8.38	3.49	8.81	1.273	1.161
c	5.00	5.4	8.6	5.4	8.38	3.49	5.79	1.273	1.161

^aThis work.^bReference 12.^cReference 15.^dReference 13.^eReference 54.^fReference 55.^gReference 56.^hReference 57.ⁱReference 58.TABLE XV. Comparison of experimental nuclear spin-rotation coupling constants of O⁷⁹BrO with those calculated from the electron spin-rotation coupling constants^a (kHz).

	experimental	calculated
C_{aa}	160.1	58.4
C_{bb}	41.6	14.1
C_{cc}	31.7	1.3

^aSee Eq. (11).

stants C_{ii} are proportional to the rotational constants B_i , one should compare the ratios Λ_{ii}^n for different molecules involving the same nuclei. The data in Table XIV indicate that the Br spin-rotation constants are strongly effected by the electro-negativity of the element to which the Br atom is bonded and that the influence of the electronic state of the molecule is less pronounced.

Endo *et al.* have proposed a relationship between the electronic and nuclear spin-rotation coupling constants to estimate the order of magnitude of the latter:⁵⁹

$$|C_{gg}/\epsilon_{gg}| = |a/A_{SO}|, \quad (11)$$

with $A_{SO} = 1312 \text{ cm}^{-1}$ the average of $A_{SO}(\text{Br})$ and $A_{SO}(\text{O})$ weighted according to the spin-density determined in Sec. IV C and $a = g_e \beta_{gN} \beta_N \langle 0 | r^{-3} | n \rangle$ approximated by $5/4T_{cc} = 977 \text{ MHz}$. The experimental values for O⁷⁹BrO and those calculated from Eq. (11) are compared in Table XV. Although in the present case the C_{ii} are larger than predicted, it appears that Eq. (11) is quite useful in indicating when the nuclear spin-rotation constants need to be considered in fitting spectra.

V. CONCLUSION

The present study of the rotational spectrum of OBrO has provided information on its molecular and electronic structure as well as an insight into its bonding. In general, OBrO fits well in the series of related compounds, such as OClO, SeO₂, and SO₂. The tendency of fourth row elements to form weaker double bonds than their third row counterparts is apparent in the relatively longer and weaker bond in OBrO compared to OClO. However, the fine and hyperfine constants indicate little change in either the electron density or the angular distribution at the halogen atom. These facts indicate that, even though the population of the π -bonding orbitals may be similar, the overlap of the $4p$ orbital on Br with the $2p$ orbital on the O atom leads to a weaker π bond than the overlap of the $3p$ orbital on Cl with the $2p$ orbital on the O atom. This is in agreement with the more general view that the tendency to form double bonds strongly decreases from the lighter to the heavier members of an element group.

The derived spectroscopic constants of OBrO allow precise predictions of its rotational spectrum well into the sub-millimeter region. In addition, these constants should be helpful in analyzing the rovibrational spectra of OBrO, particularly for the bending mode and its overtones.

ACKNOWLEDGMENTS

H.S.P.M. and C.E.M. thank the National Research Council for NASA-NRC Resident Research Associateships during this study. This research was performed at the Jet Propulsion Laboratory, California Institute of Technology, under a contract with the National Aeronautics and Space Administration.

- ¹R. P. Wayne, G. Poulet, P. Biggs, J. P. Burrows, R. A. Cox, P. J. Crutzen, G. D. Hayman, M. E. Jenkin, G. Le Bras, G. K. Moortgat, U. Platt, and R. N. Schindler, *Atmos. Environ.* **29**, 2677 (1995).
- ²M. W. Chase, *J. Phys. Chem. Ref. Data* **25**, 1069 (1996).
- ³O. V. Rattigan, R. L. Jones, and R. A. Cox, *Chem. Phys. Lett.* **230**, 121 (1994); *J. Chem. Soc. Faraday Trans.* **91**, 4189 (1995).
- ⁴D. M. Rowley, M. H. Harwood, R. A. Freshwater, and R. L. Jones, *J. Phys. Chem.* **100**, 3020 (1996).
- ⁵R. Schwarz and M. Schmeißer, *Ber. Dtsch. Chem. Ges. B* **70**, 1163 (1937).
- ⁶J. R. Byberg, *J. Chem. Phys.* **55**, 4867 (1971); **85**, 4790 (1986); J. R. Byberg and J. Linderberg, *Chem. Phys. Lett.* **33**, 612 (1975).
- ⁷D. E. Tevault, N. Walker, R. R. Smardzewski, and W. B. Fox, *J. Phys. Chem.* **82**, 2733 (1978).
- ⁸G. Maier and A. Bothur, *Z. Anorg. Allg. Chem.* **621**, 743 (1995).
- ⁹J. Kölm, A. Engdahl, O. Schrems, and B. Nelander, *Chem. Phys.* **214**, 313 (1997).
- ¹⁰N. I. Butkovskaya, I. I. Morozov, V. L. Tal'rose, and E. S. Vasiliev, *Chem. Phys.* **79**, 21 (1983).
- ¹¹C. E. Miller, S. C. Nickolaisen, J. S. Francisco, and S. P. Sander, *J. Chem. Phys.* **107**, 2300 (1997).
- ¹²E. A. Cohen, H. M. Pickett, and M. Geller, *J. Mol. Spectrosc.* **87**, 459 (1981).
- ¹³E. A. Cohen, G. A. McRae, T. L. Tan, R. R. Friedl, J. W. C. Johns, and M. Noël, *J. Mol. Spectrosc.* **173**, 55 (1995), and references therein.
- ¹⁴H. S. P. Müller, C. E. Miller, and E. A. Cohen, *Angew. Chem.* **108**, 2285 (1996); *Angew. Chem. Int. Ed. Engl.* **35**, 2129 (1996).
- ¹⁵H. S. P. Müller and E. A. Cohen, *J. Chem. Phys.* **106**, 8344 (1997).
- ¹⁶M. Birk, R. R. Friedl, E. A. Cohen, H. M. Pickett, and S. P. Sander, *J. Chem. Phys.* **91**, 6588 (1989).
- ¹⁷R. R. Friedl, M. Birk, J. J. Oh, and E. A. Cohen, *J. Mol. Spectrosc.* **170**, 383 (1995).
- ¹⁸K. Miyazaki, M. Tanoura, K. Tanaka, and T. Tanaka, *J. Mol. Spectrosc.* **116**, 435 (1986).
- ¹⁹M. Tanoura, K. Chiba, K. Tanaka, and T. Tanaka, *J. Mol. Spectrosc.* **95**, 157 (1982).
- ²⁰Y. Morino and M. Tanimoto, *J. Mol. Spectrosc.* **166**, 310 (1994).
- ²¹E. A. Alekseev, S. F. Dyubko, V. V. Ilyushin, and S. V. Podnos, *J. Mol. Spectrosc.* **176**, 316 (1996).
- ²²H. Takeo, E. Hirota, and Y. Morino, *J. Mol. Spectrosc.* **34**, 370 (1970).
- ²³E. A. Alekseev, O. I. Baskakov, S. F. Dyubko, and B. I. Polevoi, *Opt. Spektrosk.* **60**, 49 (1986) [*Opt. Spectrosc.* **60**, 30 (1986)].
- ²⁴See AIP document No. E-PAPS: E-JCPSA 107-8292 for observed transition frequencies of OBrO used in the fit, assignments and residuals. E-PAPS document files may be retrieved free of charge from our FTP server (<http://www.aip.org/epaps/epaps.html>) or from <ftp.aip.org> in the directory /epaps/. For further information: e-mail: paps@aip.org or fax: 516-576-2223.
- ²⁵R. L. Poynter and H. M. Pickett, *Appl. Opt.* **24**, 2235 (1985); H. M. Pickett, R. L. Poynter, E. A. Cohen, M. L. Delitsky, J. C. Pearson, and H. S. P. Müller, "Submillimeter, Millimeter, and Microwave Line Catalog," JPL Publication 80-23, Revision 4, Pasadena, CA, 1996.
- ²⁶J. M. Brown and T. J. Sears, *J. Mol. Spectrosc.* **75**, 111 (1979).
- ²⁷H. M. Pickett, *J. Mol. Spectrosc.* **148**, 371 (1991).
- ²⁸H. H. Brown and J. G. King, *Phys. Rev.* **142**, 53 (1966).
- ²⁹D. Patel, D. Margolese, and T. R. Dyke, *J. Chem. Phys.* **70**, 2740 (1979).
- ³⁰C. R. Parent and M. C. L. Gerry, *J. Mol. Spectrosc.* **49**, 343 (1974).
- ³¹K. Kutchitsu, *J. Chem. Phys.* **49**, 4456 (1968); K. Kutchitsu, T. Fukuyama, and Y. Morino, *J. Mol. Struct.* **1**, 463 (1968); **4**, 41 (1969).
- ³²L. F. Pacios and P. C. Gómez, *J. Phys. Chem. A* **101**, 1767 (1997).
- ³³H. Takeo, E. Hirota, and Y. Morino, *J. Mol. Spectrosc.* **41**, 420 (1972).
- ³⁴K. Tanaka and T. Tanaka, *J. Mol. Spectrosc.* **98**, 425 (1983).
- ³⁵D. Christen, *J. Mol. Struct.* **48**, 101 (1978).
- ³⁶H. S. P. Müller and H. Willner, *J. Phys. Chem.* **97**, 10589 (1993).
- ³⁷A. W. Richardson, R. W. Redding, and J. C. D. Brand, *J. Mol. Spectrosc.* **29**, 93 (1969).
- ³⁸V. P. Spiridonov and A. G. Gershikov, *J. Mol. Struct.* **140**, 173 (1986).
- ³⁹M. Sugie, M. Ayabe, H. Takeo, and C. Matsumura, *J. Mol. Struct.* **352/353**, 259 (1995).
- ⁴⁰J. B. Burkholder, P. D. Hammer, C. J. Howard, A. G. Maki, G. Thompson, and C. Chackerian, Jr., *J. Mol. Spectrosc.* **124**, 139 (1987).
- ⁴¹E. Hirota, *High-Resolution Spectroscopy of Transient Molecules* (Springer, Berlin, 1985).
- ⁴²R. N. Dixon and H. W. Kroto, *Trans. Faraday Soc.* **59**, 1484 (1963).
- ⁴³A. R. W. McKellar, *J. Mol. Spectrosc.* **86**, 43 (1981); N. Basco and R. D. Morse, *ibid.* **45**, 35 (1973).
- ⁴⁴P. R. Brown, P. B. Davies, and R. J. Stickland, *J. Chem. Phys.* **91**, 3384 (1989); T. R. Huet, C. R. Pursell, W. C. Ho, B. M. Dinelli, and T. Oka, *ibid.* **97**, 5977 (1992).
- ⁴⁵K. Kawaguchi, C. Yamada, E. Hirota, J. M. Brown, J. Buttenshaw, C. P. Parent, and T. J. Sears, *J. Mol. Spectrosc.* **81**, 60 (1980).
- ⁴⁶M. D. Marshall and A. R. W. McKellar, *J. Chem. Phys.* **85**, 3716 (1986).
- ⁴⁷A. Perrin, C. Camy-Peyret, J.-M. Flaud, and J. Kauppinen, *J. Mol. Spectrosc.* **130**, 168 (1988); A. Perrin, J.-M. Flaud, C. Camy-Peyret, B. Carli, and M. Carlotti, *Mol. Phys.* **63**, 791 (1988).
- ⁴⁸R. F. Curl, *Mol. Phys.* **9**, 585 (1965).
- ⁴⁹K. A. Peterson and H.-J. Werner, *J. Chem. Phys.* **96**, 8948 (1992).
- ⁵⁰F. J. Adrian, J. Bohandy, and B. F. Kim, *J. Chem. Phys.* **85**, 2692 (1986).
- ⁵¹J. R. Morton and K. F. Preston, *J. Magn. Reson.* **30**, 577 (1978).
- ⁵²S. Schlick and B. L. Silver, *Mol. Phys.* **26**, 177 (1973).
- ⁵³J. R. Byberg and J. Spanget-Larsen, *Chem. Phys. Lett.* **23**, 247 (1973).
- ⁵⁴H. S. P. Müller and M. C. L. Gerry, *J. Chem. Phys.* **103**, 577 (1995).
- ⁵⁵A. C. Legon and J. C. Thorn, *Chem. Phys. Lett.* **215**, 554 (1993).
- ⁵⁶C. Degli Esposti, F. Tamassia, and G. Cazzoli, *J. Mol. Spectrosc.* **163**, 313 (1994).
- ⁵⁷B. D. Osipov and M. N. Grabois, *Opt. Spektrosk.* **58**, 1150 (1985) [*Opt. Spectrosc.* **58**, 702 (1985)].
- ⁵⁸A. H. Saleck, T. Klaus, S. P. Belov, and G. Winnewisser, *Z. Naturforsch. A* **51**, 898 (1996).
- ⁵⁹Y. Endo, S. Saito, and E. Hirota, *J. Mol. Spectrosc.* **97**, 204 (1983).